



Anti-windup adaptive PID control design for a class of uncertain chaotic systems with input saturation

A.H. Tahoun^{a,b}

^a Department of Computer and Control Engineering, Faculty of Engineering, Tanta University, Tanta, Egypt

^b Department of Computer Science, Faculty of computer Science and Information Technology, Albaha University, Albaha, Saudi Arabia

ARTICLE INFO

Article history:

Received 29 June 2016

Received in revised form

2 October 2016

Accepted 5 October 2016

Available online 21 October 2016

This paper was recommended for publication by Mohammad Haeri.

Keywords:

Anti-windup

PID

Saturation

Adaptive control

Chaotic systems

Disturbances

Lyapunov's stability

ABSTRACT

In this paper, the stabilization problem of actuators saturation in uncertain chaotic systems is investigated via an adaptive PID control method. The PID control parameters are auto-tuned adaptively via adaptive control laws. A multi-level augmented error is designed to account for the extra terms appearing due to the use of PID and saturation. The proposed control technique uses both the state-feedback and the output-feedback methodologies. Based on Lyapunov's stability theory, new anti-windup adaptive controllers are proposed. Demonstrative examples with MATLAB simulations are studied. The simulation results show the efficiency of the proposed adaptive PID controllers.

© 2016 ISA. Published by Elsevier Ltd. All rights reserved.

1. Introduction

The limitations of actuators and sensors commonly cause the control input and/or measurement output to saturate. Actuator and sensor saturation affects almost all practical control systems. Specifically, while the actuators' outputs are saturated, the controlled plant operates in open-loop [1]. The typical influence of actuator saturation is a decrease in the speed of the system. However, in some cases, saturation can also prevent the system's stabilization [2]. On the other hand, the saturation of the sensor output produces an incorrect controller signal, since the actual state or output of the plant is no longer accurately measured.

Neglecting actuator and sensor saturations can consequently be the source of unwanted, even catastrophic, actions for the closed-loop system [3]. As a consequence, it is very important to develop effective robust control procedures for uncertain chaotic systems with input and output saturation [4]. In this paper, we will attempt to investigate robust adaptive PID control techniques for chaotic systems with input saturation. Recently, the problems of analysis and design of control systems with actuator and sensor saturation have been widely studied; see, for example [1–13] and the references therein.

In PID control design, some nonlinear effects must be taken into consideration in almost all controllers. Windup is a phenomenon produced by using an integral controller in systems with saturations. If a controller with an integral part is used with actuator saturation, the resulting error will continue to be integrated. This means that the integral term possibly will become very large or it will “wind up”. It is hence required that anti-windup controllers be developed [7–13].

In [8–13], with different techniques of controller design, the anti-windup gain k_b is assumed to be constant. This means that the value of it must be determined offline. The small value choice of k_b results in poor anti-windup but good tracking error, whereas the higher value choice of k_b results in good anti-windup but poor tracking error. Therefore, an optimization technique should be used in order to obtain an optimal choice of k_b that guarantees effectiveness in both anti-windup and tracking error. No work exists in the literature dealing with the online estimation of the variable k_b . This is accomplished in this paper.

Furthermore, in real applications, most of the control systems are subjected to environmental disturbances. These unpredictable disturbances may deteriorate the control performance. Robust control is necessary for systems in real world applications, when they exhibit an acceptable degree of disturbance rejection. Disturbance rejection control aims at a controller design that reduces the negative outcomes of disturbances on the control

E-mail address: alitahoun@yahoo.com

performance, and it has become a highly active research field in control systems, specially for nonlinear systems [14–16].

The presence of chaos in physical systems has been highly established and is very common. A chaotic system is an extremely nonlinear system. Due to its powerful applications in information processing, power converters, and chemical reactions, etc., it is important and practical to design a certain control law to cope with these nonlinear chaotic systems for real physical applications. To do this, several methods have been established to achieve chaotic control, see [17–34] and the reference therein.

Motivated by the above-mentioned studies, this paper proposes anti-windup adaptive PID controllers for nonlinear chaotic systems. Based on Lyapunov's stability theory, state- and output-feedback techniques are proposed to design an adaptive PID stabilizer for the chaotic systems. The proposed adaptive stabilizer assures that all the signals of the controlled system are bounded, while the states of the chaotic system converge to the equilibrium. In comparison to previous work such as [8–13], this paper has the following four advantages: 1) The weight factor for the anti-windup action k_b is considered as a variable, because of which it can be estimated online. 2) The saturated input is assumed to be unknown. 3) The system parameters matrices are assumed to be unknown. 4) The system considered here is a chaotic system that is very sensitive to the initial conditions.

In addition to the present introductory part, the rest of this paper is organized as follows: in the next section, the formulation of the problem is discussed. An anti-windup PID stabilizer with constant k_b is proposed in Section 3. Whereas, an anti-windup PID stabilizer with variable k_b is proposed in Section 4. The tracking problem is investigated in Section 4. In Section 5, an anti-windup PID stabilizer with unavailable $\text{sat}(u)$ is developed. Simulations on anti-windup controlling unified chaotic and rossler systems via adaptive PID control are carried out in Section 6. Finally, the conclusions are given in Section 7.

2. Formulation of the problem

The problem with controlling chaos is to force a chaotic system to exhibit a prefixed non-chaotic behavior and to do so robustly with respect to disturbances. To do this, we consider the following class of nonlinear single-input, single-output (SISO) systems called chaotic systems with input saturation

$$\dot{x} = Ax + f(x) + b \text{ sat}(u) + bdy = c^T x \quad (1)$$

where $x \in \mathbb{R}^n$, $u \in \mathbb{R}$, $d \in \mathbb{R}$, and $y \in \mathbb{R}$, are the system states, the control input, a bounded disturbance, and the system output, respectively, $A \in \mathbb{R}^{n \times n}$ is an unknown constant system matrix, b and $c \in \mathbb{R}^n$ are known constant matrices, (A, b) is a controllable pair, $\text{sat}(u)$ will be discussed in detail in the forthcoming section, and $f(x)$ is an unknown nonlinear function vector with $f(0) = [0, \dots, 0]^T$.

We assume there always exist positive scalars ℓ^* and d^* satisfying the following inequalities

$$\|f(x) - f(0)\| \leq \ell^* \|x\| |d| \leq d^* \quad (2)$$

where $\ell^* \leq L_1 \|b\|$ is also unknown [17]. In Eq. (2), $\|\cdot\|$ represents the vector Euclidean norm (2-norm), and $|\cdot|$ represents the scalar absolute value.

2.1. Actuator saturation

In Eq. (1), $\text{sat}(\cdot)$ is the saturation function,

$$\text{sat}(u(t)) = \begin{cases} u_{\text{upper}} & u(t) \geq u_{\text{upper}} \\ u(t) & u_{\text{lower}} < u(t) < u_{\text{upper}} \\ u_{\text{lower}} & u(t) \leq u_{\text{lower}} \end{cases} \quad (3)$$

where $u_{\text{upper}} > 0$ and $u_{\text{lower}} < 0$ are known constants defined as upper and lower plant actuator saturation values, respectively.

2.2. The objective

The objective is to design an adaptive state-feedback and PID output-feedback stabilizer for a chaotic system to generate an anti-windup bounded control input $\text{sat}(u)$, so that all signals in the system remain bounded, and $x(t)$ goes to zero as t tends to infinity.

To accomplish this, we make the following assumptions:

Assumption A1. A_m is a Hurwitz matrix satisfying $A_m^T P + PA_m = -Q$, P and Q are symmetric and positive-definite matrices, and T denotes transpose.

Assumption A2. Assume that there exists a constant vector $K_1^* \in \mathbb{R}^n$, and $k_p^*, k_b \in \mathbb{R}$ such that the following equations are satisfied

$$A_m = A + (1 - k_b)(bK_1^{*T} + bK_p^* c^T)$$

$$Pb = c$$

Remark 1. The two assumptions A1 and A2 are standard in adaptive control design. Assumption A1 represents a common strictly positive real (SPR) condition. Assumption A2 is the so-called matching condition [35,36].

2.3. Anti-windup modelling

Anti-windup compensation is to modify nominal controllers so that if the signal from the controller is different from that which enters the plant, a corrective feedback action will be employed to reduce the discrepancy [37].

Now, consider the control input, u , chosen as

$$u = u_c(t) + u_{aw}(t) \quad (4)$$

where $u_c(t)$ is the control input to be designed and $u_{aw}(t)$ the anti-windup input,

$$u_{aw}(t) = k_b(w(t) - u_c(t)) \quad (5)$$

where k_b is the weight factor for the anti-windup action and

$$w(t) = \begin{cases} u_{\text{upper}} & u \geq u_{\text{upper}} \\ u(t) & u_{\text{lower}} < u < u_{\text{upper}} \\ u_{\text{lower}} & u \leq u_{\text{lower}} \end{cases} \quad (6)$$

Now, we have two approaches to deal with the anti-windup signal $w(t)$. In the first one, $w(t)$ is considered as a bounded disturbance. In this case k_b is considered as a constant. In the second, the gain k_b is considered as a variable which can be estimated online.

3. Anti-windup PID stabilizer: k_b constant

First of all, system (1) can be rewritten as

$$\dot{x} = Ax + f(x) + bu + b\Delta u + bd \quad (7)$$

where $\Delta u = \text{sat}(u) - u(t)$.

The main stumbling block in the state dynamic Eq. (7) is the term Δu . Now, the effect of this term should be removed. One way

to remove Δu is to consider it as a disturbance. For the purpose of removing the effect of Δu , we generate Δx from the following differential equation.

$$\begin{aligned} d\Delta x/dt &= A_m \Delta x + \hat{k}_\Delta \Delta u, \\ \Delta x(0) &= 0 \end{aligned} \quad (8)$$

By defining $\tilde{k}_\Delta = b - \hat{k}_\Delta$, and an augmented error e as

$$e = x - \Delta x \quad (9)$$

and using Eqs. (7)–(9) in accordance with [Assumption A2](#), the differential equation for the dynamical error e becomes

$$\dot{e} = A_m e + f(x) + bu + \tilde{k}_\Delta \Delta u + bd - (1 - k_b) \left(bK_1^{*T} + bK_p^{*T} c^T \right) x \quad (10)$$

From Eq. (6), it can be concluded that $w(t)$ is bounded satisfying,

$$|w(t)| \leq L_2^* \quad (11)$$

where L_2^* is a constant. Therefore, the control input $u_c(t)$ is designed as

$$u_c(t) = u_{PID} + u_{classical} \quad (12)$$

The PID controller u_{PID} can be designed as

$$u_{PID} = \hat{k}_p^T y + \hat{k}_i^T \int_0^t ydt + \hat{k}_d^T \frac{d}{dt} y \quad (13)$$

where \hat{k}_p , \hat{k}_i , and $\hat{k}_d \in R$, called the PID controller gains, are the estimates of the positive constants k_p^* , k_i^* , and k_d^* , respectively.

Also, $u_{classical}$ is the part that is used to stabilize system (1) without using PID controllers,

$$\begin{aligned} u_{classical} &= \hat{K}_1^T x - \hat{L}_1 \|x\| \text{sgn}(e_1^T Pb) - \frac{k_b}{1 - k_b} \hat{L}_2 \text{sgn}(e_1^T Pb) \\ &\quad - \hat{d} \text{sgn}(e_1^T Pb) \end{aligned} \quad (14)$$

where \hat{K}_1 , \hat{L}_1 , $i = 1, 2$, and \hat{d} , called the classical controller gains, are the estimates of K_1^* , L_1^* , and d^* , respectively, and $\text{sgn}(\omega)$ indicates a sign function of ω that is defined as follows:

$$\text{sgn}(\omega) = \begin{cases} 1 & \omega > 0 \\ 0 & \omega = 0 \\ -1 & \omega < 0 \end{cases}$$

By substituting Eqs. (4), (5), and (12)–(14) into (10), we obtain

$$\begin{aligned} \dot{e} &= A_m e + f(x) + \tilde{k}_\Delta \Delta u + bd + k_b bw(t) - (1 - k_b) \left(bK_1^{*T} + bK_p^{*T} c^T \right) x \\ &\quad + (1 - k_b) b \left[\hat{K}_1^T x + \hat{k}_p y + \hat{k}_d \frac{d}{dt} y + \hat{k}_i \int_0^t ydt - \hat{L}_1 \|x\| \text{sgn}(e_1^T Pb) \right. \\ &\quad \left. - \hat{d} \text{sgn}(e_1^T Pb) - \frac{k_b}{1 - k_b} \hat{L}_2 \text{sgn}(e_1^T Pb) \right] \end{aligned}$$

Defining,

$$\tilde{K}_1 = \hat{K}_1 - K_1^*, \quad \tilde{k}_p = \hat{k}_p - k_p^*, \quad \tilde{k}_i = \hat{k}_i - k_i^*, \quad \tilde{k}_d = \hat{k}_d - k_d^* \quad (15)$$

we get

$$\begin{aligned} \dot{e} &= A_m e + f(x) + \tilde{k}_\Delta \Delta u + k_b bw(t) + bd + (1 - k_b) \\ &\quad b \left[\tilde{K}_1^T x + \tilde{k}_p y + \tilde{k}_d \frac{d}{dt} y + \tilde{k}_i \int_0^t ydt + k_d^* \frac{d}{dt} y + k_i^* \int_0^t ydt \right. \\ &\quad \left. - \hat{L}_1 \|x\| \text{sgn}(e_1^T Pb) - \hat{d} \text{sgn}(e_1^T Pb) - \frac{k_b}{1 - k_b} \hat{L}_2 \text{sgn}(e_1^T Pb) \right] \end{aligned} \quad (16)$$

Again, there are two terms in the above equation, $k_d^* \frac{d}{dt} y$ and $k_i^* \int_0^t ydt$ need to be removed. For the purpose of

removing the effect of these terms, we generate Δe from the following differential equation.

$$\Delta \dot{e} = A_{ms} \Delta e + u_e, \quad \Delta e(0) = 0 \quad (17)$$

where u_e is defined as

$$u_e = \hat{k}_{be} bw + (1 - k_b) \hat{k}_d b \frac{d}{dt} y + (1 - k_b) \hat{k}_i b \int_0^t ydt \quad (18)$$

By defining

$$\tilde{k}_{be} = k_b - \hat{k}_{be}, \quad \tilde{k}_{de} = k_d^* - \hat{k}_{de}, \quad \tilde{k}_{ie} = k_i^* - \hat{k}_{ie}, \quad (19)$$

and an augmented error e_1 as

$$e_1 = e - \Delta e \quad (20)$$

and using Eqs. (16)–(19), the differential equation for the dynamical error e_1 becomes

$$\begin{aligned} \dot{e}_1 &= A_m e_1 + f(x) + \tilde{k}_\Delta \Delta u + \tilde{k}_{be} bw + bd + (1 - k_b) \\ &\quad b \left[\tilde{K}_1^T x + \tilde{k}_p y + \tilde{k}_d \frac{d}{dt} y + \tilde{k}_i \int_0^t ydt + \tilde{k}_{de} \frac{d}{dt} y + \tilde{k}_{ie} \int_0^t ydt \right. \\ &\quad \left. - \hat{L}_1 \|x\| \text{sgn}(e_1^T Pb) - \hat{d} \text{sgn}(e_1^T Pb) - \frac{k_b}{1 - k_b} \hat{L}_2 \text{sgn}(e_1^T Pb) \right] \end{aligned} \quad (21)$$

With the knowledge above, we will propose our first result in the following theorem.

Theorem 1. Consider the chaotic system dynamic Eq. (1) satisfying [assumptions A1](#) and [A2](#). By applying the adaptive controller Eqs. (4), (5), (12), and (13) with respect to the state dynamics (21), while the unknown parameters are adapted as

$$\dot{\hat{K}}_1 = -\gamma_1 e_1^T P b x, \quad (22)$$

$$\dot{\hat{k}}_p = -\gamma_2 e_1^T P b y, \quad (23)$$

$$\dot{\hat{k}}_i = \dot{\hat{k}}_{ie} = -\gamma_3 e_1^T P b \int_0^t ydt, \quad (24)$$

$$\dot{\hat{k}}_d = \dot{\hat{k}}_{de} = -\gamma_4 e_1^T P b \frac{d}{dt} y, \quad (25)$$

$$\dot{\hat{k}}_\Delta = -\gamma_5 e_1^T P \Delta u, \quad (26)$$

$$\dot{\hat{k}}_{be} = -\gamma_6 e_1^T P b w, \quad (27)$$

$$\dot{\hat{L}}_1 = \gamma_7 |e_1^T P b| \|x\|, \quad (28)$$

$$\dot{\hat{L}}_2 = \gamma_8 |e_1^T P b|, \quad (29)$$

$$\dot{\hat{d}} = \gamma_9 |e_1^T P b|, \quad (30)$$

where $\tilde{L}_i = \hat{L}_i - L_i^*$, $i = 1, 2$, and γ_j , $j = 1, \dots, 9$, are positive constant

gains, it is shown that the closed-loop system dynamics are stable and the states, x , converge to zero.

Proof. With $0 < k_b < 1$, we consider the following positive-definite Lyapunov function $V(t)$,

$$V = e_1^T P e_1 + (1 - k_b) \gamma_1^{-1} \tilde{K}_1^T \tilde{K}_1 + (1 - k_b) \gamma_2^{-1} \tilde{k}_p^2 + (1 - k_b) \gamma_3^{-1} \tilde{k}_l^2 + (1 - k_b) \gamma_4^{-1} \tilde{k}_D^2 + (1 - k_b) \gamma_5^{-1} \tilde{k}_{De}^2 + (1 - k_b) \gamma_6^{-1} \tilde{k}_\Delta^T \tilde{k}_\Delta + \gamma_6^{-1} \tilde{k}_{be}^2 + (1 - k_b) \gamma_7^{-1} \tilde{L}_1^2 + k_b \gamma_8^{-1} \tilde{L}_2^2 + (1 - k_b) \gamma_9^{-1} \tilde{d}^2 \quad (31)$$

Taking the time derivative of the Lyapunov function (31) along system (1), we have

$$\dot{V} = e_1^T P \dot{e}_1 + e_1^T P \dot{e}_1 + 2(1 - k_b) \gamma_1^{-1} \tilde{K}_1^T \dot{\tilde{K}}_1 + 2(1 - k_b) \gamma_2^{-1} \tilde{k}_p \dot{\tilde{k}}_p + 2(1 - k_b) \gamma_3^{-1} \tilde{k}_l \dot{\tilde{k}}_l + 2(1 - k_b) \gamma_4^{-1} \tilde{k}_D \dot{\tilde{k}}_D + 2\gamma_5^{-1} \tilde{k}_\Delta^T \dot{\tilde{k}}_\Delta + 2\gamma_6^{-1} \tilde{k}_{be} \dot{\tilde{k}}_{be} + 2(1 - k_b) \gamma_7^{-1} \tilde{L}_1 \dot{\tilde{L}}_1 + 2\gamma_8^{-1} k_b \tilde{L}_2 \dot{\tilde{L}}_2 + 2(1 - k_b) \gamma_9^{-1} \tilde{d} \dot{\tilde{d}} + 2(1 - k_b) \gamma_4^{-1} \tilde{k}_{De} \dot{\tilde{k}}_{De} + 2(1 - k_b) \gamma_3^{-1} \tilde{k}_{le} \dot{\tilde{k}}_{le} \quad (32)$$

Substituting (22)–(30) into (32), it can be concluded that

$$\dot{V} = -e_1^T Q e_1 + 2e_1^T P f(x) + 2e_1^T P b d + 2(1 - k_b) e_1^T P b \left[-\hat{L}_1 \|x\| \text{sgn}(e_1^T P b) - \frac{k_b}{1 - k_b} \hat{L}_2 \text{sgn}(e_1^T P b) - \hat{d} \text{sgn}(e_1^T P b) \right] + 2(1 - k_b) \left[\tilde{L}_1 |e_1^T P b| \|x\| + \tilde{d} |e_1^T P b| + \frac{k_b}{1 - k_b} \tilde{L}_2 |e_1^T P b| \right]$$

Again, using (2), Assumptions A1 and A2, and the fact

$$e_1^T P b \text{sgn}(e_1^T P b) = |e_1^T P b|$$

Finally, we get

$$\dot{V} \leq -x^T Q x$$

Consequently, we can conclude that the closed-loop system is stable based on the Lyapunov stability theory. This completes the proof.

Remark 2. Theorem 1 assumes that k_b is constant as in [8–13] and needs to be determined offline. This restriction can be relaxed by considering k_b a variable that can be estimated online. The advantage of this consideration will be demonstrated in the following section.

4. Anti-windup PID stabilizer: k_b variable

In this section, we consider the class of nonlinear single-input, single-output (SISO) systems (1) with input saturation. By considering k_b as a controller gain, Assumption A2 need to be modified as:

Assumption A3: Assume that there exists a constant vector $K_1^* \in \mathbb{R}^n$, and $k_p^* \in \mathbb{R}$ such that the following equations are satisfied.

$$A_m = A + (b K_1^{*T} + b K_p^{*T} c^T) x$$

$$p b = c$$

Remark 3. Assumptions A3 is a modified version of assumption A2 as k_b is variable.

By assuming k_b as variable, Eq. (4) can be rewritten as

$$u_{aw}(t) = \hat{k}_b(w(t) - u_c(t)) \quad (33)$$

Here, the control input $u_c(t)$ is designed as in (12) with u_{PID} as in (13) and

$$u_{classical} = \hat{K}_1^T x - \hat{L}_1 \|x\| \text{sgn}(e^T P b) - \hat{d} \text{sgn}(e^T P b) \quad (34)$$

By substituting (33), (13), and (34), into (7), taking into consideration Assumption A3, we obtain

$$\begin{aligned} \dot{x} = & A_m x + f(x) + b d + b \Delta u + \tilde{k}_b b(w - u_c) + b \tilde{K}_1^T x + b \tilde{k}_p y \\ & + b \tilde{k}_D \frac{d}{dt} y + b \tilde{k}_l \int_0^t y dt - b \hat{L}_1 \|x\| \text{sgn}(e^T P b) - b \hat{d} \text{sgn}(x^T P b) \\ & + k_l^* \int_0^t y dt + k_D^* \frac{d}{dt} y + k_p^* y + k_b b(w - u_c) \end{aligned} \quad (35)$$

where $\tilde{k}_b = \hat{k}_b - k_b$.

In (35), there are many terms that need to be removed. In the same way as in the previous section, we generate Δx from the following differential equation.

$$\Delta \dot{x} = A_m \Delta x + u_x, \Delta x(0) = 0 \quad (36)$$

where u_x is defined as

$$u_x = \hat{k}_\Delta \Delta u + \hat{k}_{px} b y + \hat{k}_{lx} b \int_0^t y dt + \hat{k}_{Dx} b \frac{d}{dt} y + \hat{k}_b b(w - u_c) \quad (37)$$

By defining

$$\tilde{k}_\Delta = b - \hat{k}_\Delta, \tilde{k}_{bx} = k_b - \hat{k}_{bx}, \tilde{k}_{Dx} = k_D^* - \hat{k}_{Dx}, \tilde{k}_{lx} = k_l^* - \hat{k}_{lx}, \quad (38)$$

and an augmented error e as

$$e = x - \Delta x \quad (39)$$

and using (35)–(37) and (39), the differential equation for the dynamical error e becomes

$$\begin{aligned} \dot{e} = & A_m e + f(x) + \tilde{k}_\Delta \Delta u + b d + \tilde{k}_b b(w - u_c) + b \tilde{K}_1^T x + b \tilde{k}_p y \\ & + b \tilde{k}_D \frac{d}{dt} y + b \tilde{k}_l \int_0^t y dt - b \hat{L}_1 \|x\| \text{sgn}(e^T P b) - b \hat{d} \text{sgn}(x^T P b) \\ & + b \tilde{k}_{px} y + b \tilde{k}_{Dx} \frac{d}{dt} y + b \tilde{k}_{lx} \int_0^t y dt \end{aligned} \quad (40)$$

With the knowledge above, we will propose the second result in the following theorem.

Theorem 2. Consider the chaotic system dynamic (1) satisfying assumptions A1 and A3 subjected to input saturation. By applying the adaptive controller (33) and (34) with respect to the state dynamics (40) while the unknown parameters are adapted as

$$\dot{\hat{K}}_1 = -\alpha_1 e^T P b x, \quad (42)$$

$$\dot{\hat{k}}_p = -\alpha_2 e^T P b y, \quad (43)$$

$$\dot{\hat{k}}_l = \dot{\hat{k}}_{lx} = -\alpha_3 e^T P b \int_0^t y dt, \quad (44)$$

$$\dot{\hat{k}}_D = \dot{\hat{k}}_{Dx} = -\alpha_4 e^T P b \frac{d}{dt} y, \quad (45)$$

$$\dot{\hat{k}}_\Delta = -\alpha_5 e^T P \Delta u, \quad (46)$$

$$\dot{\tilde{k}}_{px} = -\alpha_6 e^T P b \quad y, \quad (47)$$

$$\dot{\tilde{k}}_b = -\alpha_7 e^T P b (w - u_c), \quad (48)$$

$$\dot{\tilde{L}}_1 = \alpha_8 |e^T P b| \|x\|, \quad (49)$$

$$\dot{\tilde{d}} = \alpha_9 |e^T P b|, \quad (50)$$

where $\alpha_j, j=1, \dots, 9$, are positive constant gains, it is shown that the closed-loop system dynamics are stable and the states, x , converge to zero.

Proof. Consider the following positive-definite Lyapunov function $V(t)$,

$$V = e^T P e + \alpha_1^{-1} \tilde{K}_1^T \tilde{K}_1 + \alpha_2^{-1} \tilde{k}_p^2 + \alpha_3^{-1} \tilde{k}_l^2 + \alpha_4^{-1} \tilde{k}_D^2 + \alpha_5^{-1} \tilde{k}_d^T \tilde{k}_d + \alpha_6^{-1} \tilde{k}_{px}^2 + \alpha_7^{-1} \tilde{k}_b^2 + \alpha_8^{-1} \tilde{L}_1^2 + \alpha_9^{-1} \tilde{d}^2 + \alpha_3^{-1} \tilde{k}_{lx}^2 + \alpha_4^{-1} \tilde{k}_{Dx}^2 \quad (51)$$

Taking the time derivative of the Lyapunov function (51) along system (1), we have

$$\begin{aligned} \dot{V} = & \dot{e}^T P e + e^T P \dot{e} + 2 + \alpha_1^{-1} \tilde{K}_1^T \dot{\tilde{K}}_1 + 2\alpha_2^{-1} \tilde{k}_p \dot{\tilde{k}}_p + 2\alpha_3^{-1} \tilde{k}_l \dot{\tilde{k}}_l \\ & + 2\alpha_4^{-1} \tilde{k}_D \dot{\tilde{k}}_D + 2\alpha_5^{-1} \tilde{k}_d^T \dot{\tilde{k}}_d + 2\alpha_6^{-1} \tilde{k}_{px} \dot{\tilde{k}}_{px} + 2\alpha_7^{-1} \tilde{k}_b \dot{\tilde{k}}_b + 2\alpha_8^{-1} \tilde{L}_1 \dot{\tilde{L}}_1 \\ & + 2\alpha_9^{-1} \tilde{d} \dot{\tilde{d}} + 2\alpha_3^{-1} \tilde{k}_{lx} \dot{\tilde{k}}_{lx} + 2\alpha_4^{-1} \tilde{k}_{Dx} \dot{\tilde{k}}_{Dx} \end{aligned} \quad (52)$$

Substituting (42)–(50) into (52), using (2), assumption A1 and A3, it can be finally found that

$$\dot{V} \leq -x^T Q x$$

Subsequently, it can be concluded that the closed-loop system is stable based on the Lyapunov stability theory. This completes the proof.

Remark 4. The above approach can easily be modified for the tracking problem. A model reference control approach can be investigated by considering a reference model described by the state-space equations.

$$\dot{x}_m = A_m x_m + b_m r y_m = c^T x_m$$

where $x_m \in \mathbb{R}^n$ is a state vector, $r \in \mathbb{R}^n$ is a piecewise continuous, uniformly bounded reference input. The reference model matrices A_m , b_m , and c are known with compatible dimensions. The objective is to design a model reference direct state feedback and PID output feedback adaptive controller for the chaotic system (1) in which adaptive control laws are synthesized in such a way that the output error e , $e = x - x_m$, satisfies $\lim_{t \rightarrow \infty} e = 0$, for all $t \geq 0$.

5. Anti-windup PID stabilizer: $\text{sat}(u)$ is not available

In the previous sections, we assumed that $\text{sat}(u)$ is available for measurement. In this section, the case of $\text{sat}(u)$ not being available for measurement is considered.

In view of (7), it can be rewritten as

$$\dot{x} = A x + f(x) + b u + b \text{sat}(u) - b u + b d \quad (53)$$

Now, $\text{sat}(u)$ is not available for measurement, therefore it can be considered as a disturbance. From (3), it can be found that

$$|\text{sat}(u)| \leq L_2^* \quad (54)$$

Using the assumptions A1 and A3 and the same controller as in (33) and (13), using

$$u_{\text{classical}} = \hat{K}_1^T x - \hat{L}_1 \|x\| \text{sgn}(e^T P b) - \hat{L}_2 \text{sgn}(e^T P b) - \hat{d} \text{sgn}(e^T P b) \quad (55)$$

By substituting (33), (13), and (55), into (53), we obtain

$$\begin{aligned} \dot{x} = & A_m x + f(x) + b d + b \text{sat}(u) - b u + \tilde{k}_b (w - u_c) + b \tilde{K}_1^T x \\ & + b \tilde{k}_p y + b \tilde{k}_D \frac{d}{dt} y + b \tilde{k}_l \int_0^t y dt - b \hat{L}_1 \|x\| \text{sgn}(e^T P b) \\ & - b \hat{d} \text{sgn}(x^T P b) + k_l^* \int_0^t y dt + k_D^* \frac{d}{dt} y + k_p^* y + k_b (w - u_c) \end{aligned} \quad (56)$$

In (56), there are many terms that need to be removed. In the same way as in the previous section, we generate Δx from the following differential equation.

$$\Delta \dot{x} = A_m \Delta x + u_x, \quad \Delta x(0) = 0 \quad (57)$$

where u_x is defined as

$$u_x = -\hat{k}_d u + \hat{k}_{px} b y + \hat{k}_{lx} b \int_0^t y dt + \hat{k}_{Dx} b \frac{d}{dt} y + \hat{k}_b b (w - u_c) \quad (58)$$

By defining

$$\tilde{k}_d = \hat{k}_d - b, \quad \tilde{k}_{bx} = k_b - \hat{k}_{bx}, \quad \tilde{k}_{Dx} = k_D^* - \hat{k}_{Dx}, \quad \tilde{k}_{lx} = k_l^* - \hat{k}_{lx}, \quad (59)$$

and an augmented error e as

$$e = x - \Delta x \quad (60)$$

and using (56)–(60), the differential equation for the dynamical error e becomes

$$\begin{aligned} \dot{e} = & A_m e + f(x) + \tilde{k}_d u + b \text{sat}(u) + \tilde{k}_b b (w - u_c) + b \tilde{K}_1^T x + b \tilde{k}_p y \\ & + b \tilde{k}_D \frac{d}{dt} y + b \tilde{k}_l \int_0^t y dt - b \hat{L}_1 \|x\| \text{sgn}(e^T P b) - b \hat{d} \text{sgn}(x^T P b) \\ & + b \tilde{k}_{px} y + b \tilde{k}_{Dx} \frac{d}{dt} y + b \tilde{k}_{lx} \int_0^t y dt + b d \end{aligned} \quad (61)$$

With the knowledge above, we will propose the second result in the following theorem.

Theorem 3. Consider the chaotic system dynamic(1) satisfying assumptions A1 and A3 subjected to input saturation. By applying the adaptive controller (33), (13), (56) with respect to the state error dynamics (61) while the unknown parameters are adapted as in (42)–(50) with replacing Δu by u in (46) in addition to

$$\dot{\tilde{L}}_2 = \alpha_{10} |e^T P b|, \quad (62)$$

where α_{10} is a positive constant gain, it is shown that the closed-loop system dynamics are stable and the states, x , converge to zero.

Proof. Consider the following positive-definite Lyapunov function $V(t)$,

$$\begin{aligned} V = & e^T P e + \alpha_1^{-1} \tilde{K}_1^T \tilde{K}_1 + \alpha_2^{-1} \tilde{k}_p^2 + \alpha_3^{-1} \tilde{k}_l^2 + \alpha_4^{-1} \tilde{k}_D^2 + \alpha_5^{-1} \tilde{k}_d^T \tilde{k}_d \\ & + \alpha_6^{-1} \tilde{k}_{px}^2 + \alpha_7^{-1} \tilde{k}_b^2 + \alpha_8^{-1} \tilde{L}_1^2 + \alpha_9^{-1} \tilde{d}^2 + \alpha_3^{-1} \tilde{k}_{lx}^2 + \alpha_4^{-1} \tilde{k}_{Dx}^2 \\ & + \alpha_{10}^{-1} \tilde{L}_2^2 \end{aligned} \quad (63)$$

Taking the time derivative of the Lyapunov function (63) along system (1), we have

$$\begin{aligned} \dot{V} = & e^T P e + e^T P \dot{e} + 2 + \alpha_1^{-1} \dot{\tilde{K}}_1^T \dot{\tilde{K}}_1 + 2\alpha_2^{-1} \dot{\tilde{K}}_P^T \dot{\tilde{K}}_P + 2\alpha_3^{-1} \dot{\tilde{K}}_I^T \dot{\tilde{K}}_I \\ & + 2\alpha_4^{-1} \dot{\tilde{K}}_D^T \dot{\tilde{K}}_D + 2\alpha_5^{-1} \dot{\tilde{K}}_A^T \dot{\tilde{K}}_A + 2\alpha_6^{-1} \dot{\tilde{K}}_{PX}^T \dot{\tilde{K}}_{PX} + 2\alpha_7^{-1} \dot{\tilde{K}}_b^T \dot{\tilde{K}}_b + 2\alpha_8^{-1} \dot{\tilde{L}}_1^T \dot{\tilde{L}}_1 \\ & + 2\alpha_9^{-1} \dot{\tilde{d}}^T \dot{\tilde{d}} + 2\alpha_3^{-1} \dot{\tilde{K}}_{IX}^T \dot{\tilde{K}}_{IX} + 2\alpha_4^{-1} \dot{\tilde{K}}_{DX}^T \dot{\tilde{K}}_{DX} \end{aligned} \quad (64)$$

Finally, it can be finally concluded that

$$\dot{V} \leq -x^T Q x$$

As a result, it can be accomplished that the closed-loop system is stable based on the Lyapunov stability theory. This completes the proof.

6. Numerical results

In this section, anti-windup PID controllers will be simulated. Based on [Theorems 1–3](#), we will design the adaptive feedback controller. The simulation results will show that the proposed controllers are feasible and valid.

Example 1. As we know, many chaotic systems investigated are in the form (1) such as the unified chaotic system [17]. The unified chaotic system is

$$\begin{aligned} \dot{x}_1 &= (25\alpha + 10)(x_2 - x_1)\dot{x}_2 = (28 - 35\alpha)x_1 - x_1x_3 + (29\alpha - 1)x_2\dot{x}_3 \\ &= x_1x_2 - \frac{\alpha + 8}{3}x_3 \end{aligned}$$

where $\alpha \in [0, 1]$. When $\alpha \in [0, 0.8]$ it is a Lorenz chaotic system, $\alpha = 0.8$ is a Lu chaotic system [8], and $\alpha \in (0.8, 1]$ is a Chen system. For the unified chaotic system, let

$$\begin{aligned} A &= \begin{bmatrix} -10 & 10 & 0 \\ 28 & -1 & 0 \\ 0 & -1 & -8/3 \end{bmatrix}, \quad b = \begin{bmatrix} 1 \\ 1 \\ 0 \end{bmatrix}, \quad c = \begin{bmatrix} 1 \\ 1 \\ 0 \end{bmatrix}, \\ f(x) &= \begin{bmatrix} 25\alpha(x_2 - x_1) \\ -35\alpha x_1 + 29\alpha x_2 - x_1x_3 \\ (x_1 - 1)x_2 - \alpha x_3/3 \end{bmatrix}, \quad d = 0.1 \sin t \end{aligned}$$

we assume that A , $f(x)$ and the parameter α are not known. Based on [Theorem 1](#), we assume $P=I$ ($n \times n$ Identity matrix), $A_m = -I$, the simulation results are shown in [Figs. 1–5](#). The anti-windup robust chaotic behaviors of the PID adaptive stabilizer with constant k_b are shown in [Figs. 1–3](#). The anti-windup robust

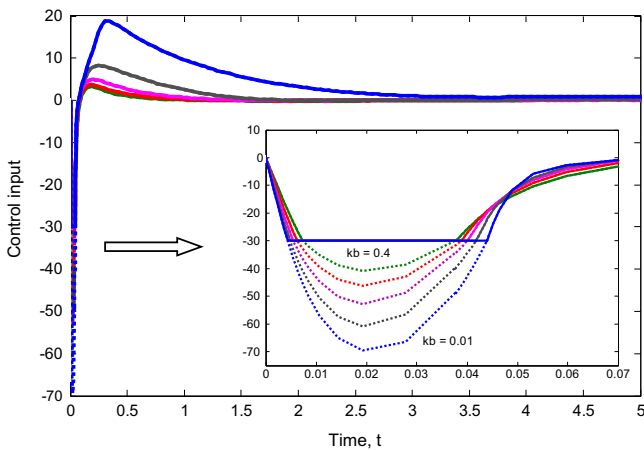


Fig. 1. The control input and the saturated input with different values of k_b , $u = -u_{\text{lower}} = 30$. (Dotted: the control input, solid: the saturated input). (The controller is applied at $t=0$).

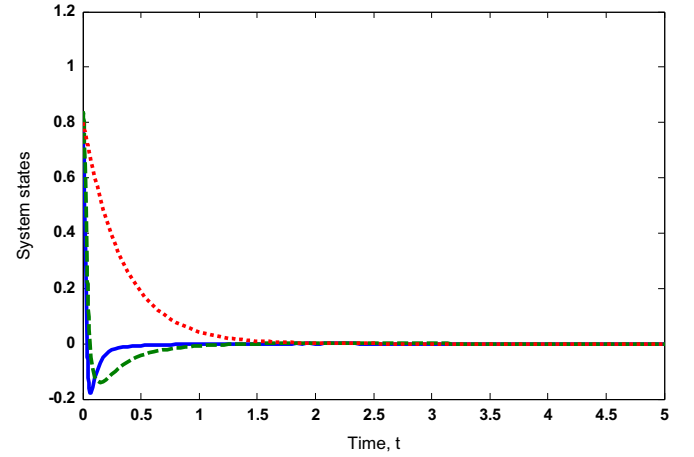


Fig. 2. The system states, $k_b = 0.3$, $u_{\text{upper}} = -u_{\text{lower}} = 30$. (Dashed: x_1 , solid: x_2 , dotted: x_3). (The controller is applied at $t=0$).

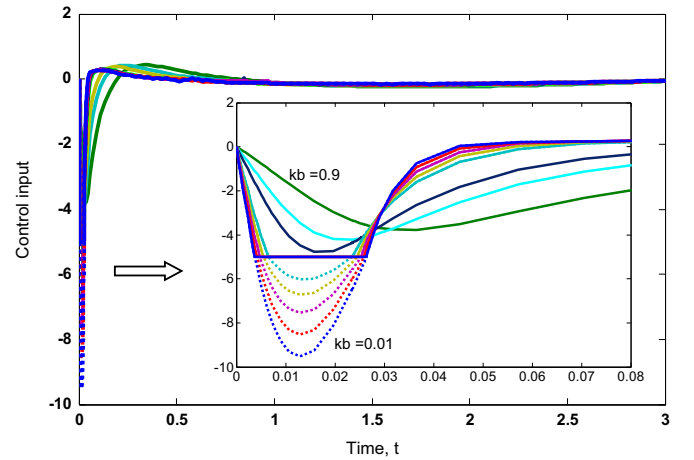


Fig. 3. The control input and the saturated input with different values of k_b , $u_{\text{upper}} = -u_{\text{lower}} = 5$. (Dotted: the control input, solid: the saturated input). (The controller is applied at $t=0$).

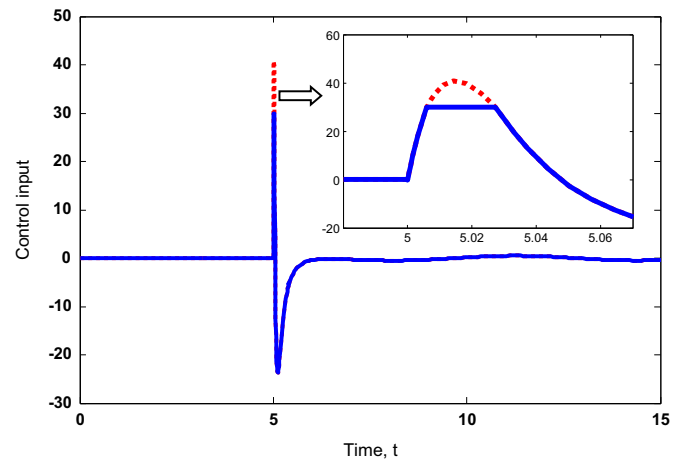


Fig. 4. The control input and the saturated input, k_b is estimated online, $u_{\text{upper}} = -u_{\text{lower}} = 30$. (Dotted: the control input, solid: the saturated input). (The controller is applied at $t=5$).

chaotic behaviors of the PID adaptive stabilizer with variable k_b are variable, as shown in [Figs. 4 and 5](#).

[Figs. 1 and 3](#) depict the generated control input trajectories for different values of $0 < k_b < 1$ and the saturated control input. The saturation level is set to ± 30 and ± 5 , respectively. However, the

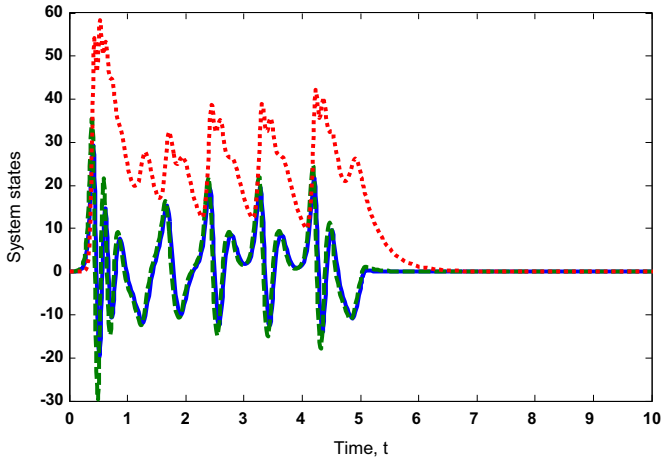


Fig. 5. The system states, k_b is estimated online, $u_{upper}=-u_{lower}=30$. (Dashed: x_1 , solid: x_2 , dotted: x_3). (The controller is applied at $t=5$).

proposed adaptive anti-windup method guarantees the system state tracking as shown in Fig. 2. It is to be noted that, as shown in Figs. 1 and 3, if $k_b=0$ then a windup may occur. If $k_b=1$, there is no matching condition, according to assumption A2, and the stability of the system is not guaranteed. As k_b increases, the proposed anti-windup controller becomes very effective and both the saturated and unsaturated inputs become equal but the performance of the state tracking may be poor but still stable. This problem is solved in Figs. 4 and 5, with variable k_b .

Example 2. Consider the Rossler chaotic system [38]:

$$\dot{x}_1 = -x_2 - x_3$$

$$\dot{x}_2 = x_1 + 0.2$$

$$x_2 \dot{x}_3 = 0.2 + x_3(x_1 - 5.7)$$

This can be written as in (1) where

$$A = \begin{bmatrix} 0 & -1 & -1 \\ 1 & 0.2 & 0 \\ 0 & 0 & -5.7 \end{bmatrix}, \quad b = \begin{bmatrix} 1 \\ 0 \\ 1 \end{bmatrix}, \quad f(x) = \begin{bmatrix} 0 \\ 0 \\ 0.2 + x_3 x_1 \end{bmatrix}, \quad d = 0.1 \sin t$$

The simulation results are shown in Figs. 6–11. The anti-windup robust chaotic behaviors of the PID adaptive stabilizer with constant k_b are shown in Figs. 6–9. The anti-windup robust chaotic behaviors of the PID adaptive stabilizer with variable k_b are

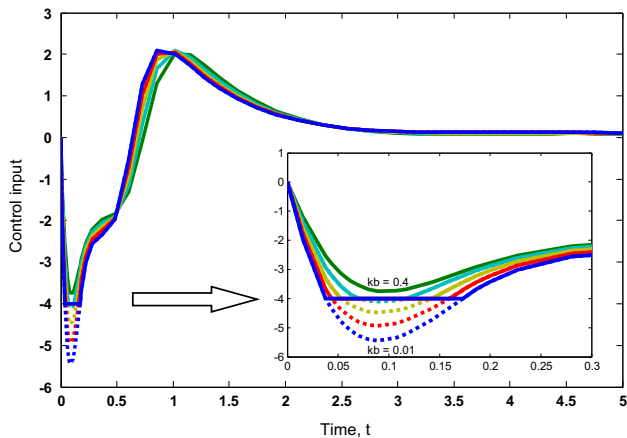


Fig. 6. The control input and the saturated input with different values of k_b , $u_{upper}=-u_{lower}=4$. (Dotted: the control input, solid: the saturated input). (The controller is applied at $t=0$).

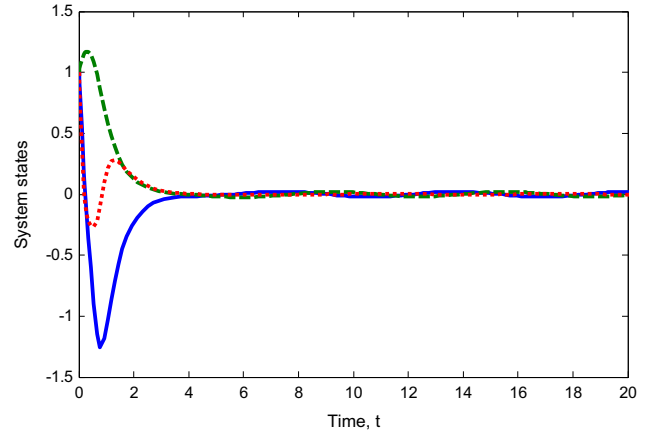


Fig. 7. The system states, $k_b=0.1$, $u_{upper}=-u_{lower}=4$. (Dashed: x_1 , solid: x_2 , dotted: x_3). (The controller is applied at $t=0$).

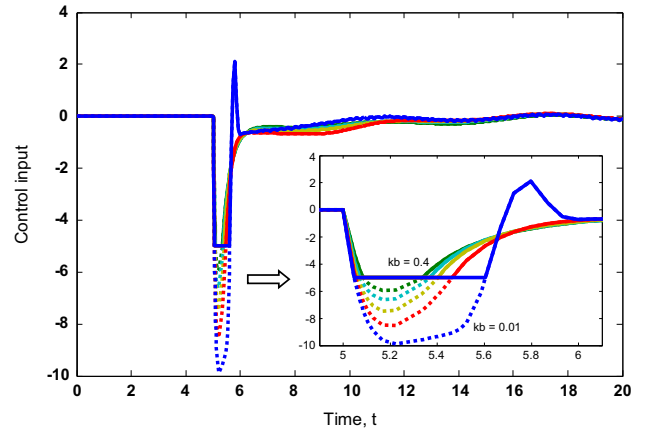


Fig. 8. The control input and the saturated input with different values of k_b , $u_{upper}=-u_{lower}=5$. (Dotted: the control input, solid: the saturated input). (The controller is applied at $t=5$).

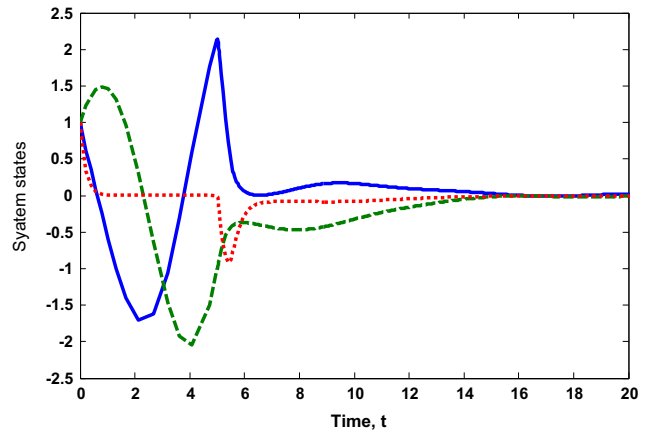


Fig. 9. The system states, $k_b=0.1$, $u_{upper}=-u_{lower}=5$. (Dashed: x_1 , solid: x_2 , dotted: x_3). (The controller is applied at $t=5$).

variable, as shown in Figs. 10 and 11.

Remark 5. In the simulation results shown in Figs. 4, 5, and 8–11 we did not apply our controller at $t=0$, to show the dynamics of the controller-free chaotic system. We start to apply our controller by random at $t=5$ in Figs. 4, 5, 8 and 9 and at $t=10$ in Figs. 10 and 11. The choice of this time is insignificant.

Remark 6. Comparing Examples 1 and 2, it is to be noted that, the

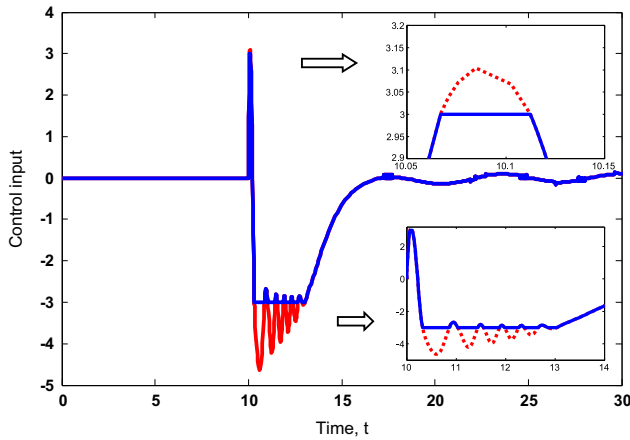


Fig. 10. The control input and the saturated input, k_b is estimated online, $u_{\text{upper}} = -u_{\text{lower}} = 3$. (Dotted: the control input, solid: the saturated input). (The controller is applied at $t = 10$).

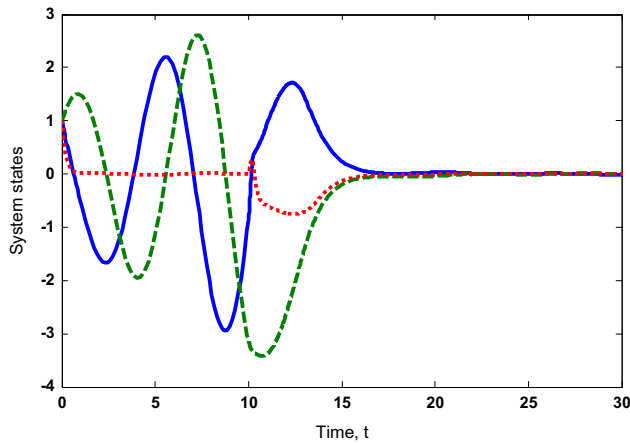


Fig. 11. The system states, k_b is estimated online, $u_{\text{upper}} = -u_{\text{lower}} = 3$. (Dashed: x_1 , solid: x_2 , dotted: x_3). (The controller is applied at $t = 10$).

dynamic of the unified chaotic systems presented in Example 1 is higher than the Rossler chaotic system presented in Example 2. Therefore, the saturation levels in the first example are higher than that in the second example.

Remark 7. In view of previous work such as [8–13], the constant k_b needs an additional optimization technique to find its appropriate value. These optimization techniques need to be carried out offline. In our approach, the value of k_b is estimated online. This makes our work advantageous.

Remark 8. In the above two examples, we apply our first algorithm proposed in Section 3 with the assumption that k_b is constant (all previous work consider this assumption such as [8–13] but for completely known system parameters). This is shown in Figs. 1–3 for Example 1 and Figs. 6–9 for Example 2. Also, the main contribution of this paper investigated in Section 4 with the assumption that k_b is variable and unknown is applied in the same above two examples. This is shown in Figs. 4 and 5 for Example 1 and Figs. 10 and 11 for Example 2. We apply the two proposed approaches in the same examples with the same parameters to show the advantages and the effectiveness of our work.

7. Conclusions

This paper addresses methodologies for suppressing chaos in nonlinear systems in the presence of actuator saturation and

uncertainty. Using PID with saturation may results in a windup. In this paper, anti-windup stabilizers are achieved. A multi-level augmented error is designed to account for the extra terms appearing due to the use of PID and saturation. Based on Lyapunov's stability theory, adaptive control laws are synthesized. Illustrative examples with numerical simulations are carried out. The results confirm the significance of the proposed control techniques.

References

- [1] Lin Z, Hu T. Semi-global stabilization of linear systems subject to output saturation. In: Proceedings of the 39th IEEE conference on decision and control. Sydney, Australia; 2000.
- [2] Paiva HM, Galvão RKH. Simulation of dynamic systems with output saturation. IEEE Trans Educ 2004;47:385–8.
- [3] Garcia G, Tarbouriech S, Gomes da Silva Jo-ao Manoel Jr. Dynamic output controller design for linear systems with actuator and sensor saturation. In: Proceedings of the 2007 American control conference. Times Square New York City, USA: Marriott Marquis Hotel; 2007. p. 11–13.
- [4] Chen M, Tao G, Jiang B. Dynamic surface control using neural networks for a class of uncertain nonlinear systems with input saturation. IEEE Trans Neural Netw Learn Syst 2014;26:2086–97.
- [5] Ran M, Wang Q, Dong C. Stabilization of a class of nonlinear systems with actuator saturation via active disturbance rejection control. Automatica 2016;63:302–10.
- [6] Matthew CT, Sophie T. Anti-windup for linear systems with sensor saturation: sufficient conditions for global stability and L2 gain. In: Proceedings of the 45th IEEE conference on decision & control. USA; 2006.
- [7] Åström KJ, Murray RM. Feedback systems: an introduction for scientists and engineers. New Jersey: Princeton University Press; 2008 [ISBN: 9780691135762].
- [8] Ran M, Wang Q, Dong C. Anti-windup design for uncertain nonlinear systems subject to actuator saturation and external disturbance. Int J Robust Nonlinear Control 2016. <http://dx.doi.org/10.1002/rnc.3524>.
- [9] Gomes da Silva Jr. JM, Oliveira MZ, Coutinho D, Tarbouriech S. Static anti-windup design for a class of nonlinear systems. Int J Robust Nonlinear Control 2014;24:793–810.
- [10] Ting C-S, Chang Y-N. Robust anti-windup controller design of time-delay fuzzy systems with actuator saturations. Inf Sci 2011;181:3225–45.
- [11] Ting C-S, Liu C-S. Stabilization of nonlinear time-delay systems with input saturation via anti-windup fuzzy design. Soft Comput 2011;15:877–88.
- [12] Oliveira MZ, Gomes da Silva Jr. JM, Coutinho D, Tarbouriech S. Design of anti-windup compensators for a class of nonlinear control systems with actuator saturation. J Control Autom Electr Syst 2013;24:212–22.
- [13] Mercorelli P. An optimal and stabilising PI controller with an anti-windup scheme for a purification process of potable water. IFAC-PapOnline 2015;48 (25):259–64.
- [14] Alago BB, Keles C, Tan N. Disturbance rejection performance analyses of closed loop control systems by reference to disturbance ratio. ISA Trans 2015;55:63–71.
- [15] Liu R-J, Liu G-P, Wu M, Shed J, Nie Z-Y. Robust disturbance rejection in modified repetitive control system. Syst Control Lett 2014;70:100–8.
- [16] Yao X, Guo L. Disturbance attenuation and rejection for discrete-time Markovian jump systems with lossy measurements. Inf Sci 2014;278:673–84.
- [17] Telo-Cuautle E, Carbajal-Gomez VH, Carbajal-Gomez G. A survey on the integrated design of chaotic oscillators. Appl Math Comput 2013;219:5113–22.
- [18] Poursamad A, Markazi HD. Adaptive fuzzy sliding-mode control for multi-input multi-output chaotic systems. Chaos Solitons Fractals 2009;42:3100–9.
- [19] Adloo H, Noroozi N, Karimaghadeh P. Observer-based model reference adaptive control for unknown time-delay chaotic systems with input nonlinearity. Nonlinear Dyn 2012;67:1337–56.
- [20] Yau HT, Chen CL. Chaos control of Lorenz systems using adaptive controller with input saturation. Chaos Solitons Fractals 2007;34:1567–74.
- [21] Peng CC, Chen CL. Robust chaotic control of Lorenz system by backstepping design. Chaos Solitons Fractals 2008;37:598–608.
- [22] Chen G. A simple adaptive feedback control method for chaos and hyperchaos control. Appl Math Comput 2011;217:7258–64.
- [23] Noroozi N, Roopaei M, Karimaghadeh P, Safavi AA. Simple adaptive variable structure control for unknown chaotic systems. Commun Nonlinear Sci Numer Simul 2010;15:707–27.
- [24] Zhang H, Liu D, Wang Z. Feedback control of chaotic systems. Control Chaos Synchron Chaotification 2009:103–31.
- [25] Tahoun AH. Adaptive actuator failure compensation design for unknown chaotic multi-input systems. Int J Adapt Control signal Process 2015;29:1328–40.
- [26] Tahoun AH. Adaptive stabilizer for chaotic networked systems with network induced delays and packet losses. Nonlinear Dyn 2015;81:823–32.
- [27] Leipo L, Jiexin P, Xiaona S, Zhumu F, Xiaohong W. Adaptive sliding mode control of uncertain chaotic systems with input nonlinearity. Nonlinear Dyn 2014;76:1857–65.
- [28] Yuming C, Qigui Y. Dynamics of a hyperchaotic Lorenz-type system. Nonlinear

- Dyn 2014;77:569–81.
- [29] Xiangtao L, Minghao Y. Parameter estimation for chaotic systems by hybrid differential evolution algorithm and artificial bee colony algorithm. *Nonlinear Dyn* 2014;77:61–71.
 - [30] Rosario T, Patrick L. Robust PID controller tuning based on the heuristic Kalman algorithm. *Automatica* 2009;45:2099–106.
 - [31] Amin H-A, Hao Y. Structural analysis of fuzzy controllers with nonlinear input fuzzy sets in relation to nonlinear PID control with variable gains. *Automatica* 2004;40:1551–9.
 - [32] Davendra D, Zelinka I, Senkerik R. Chaos driven evolutionary algorithms task PID control. *Comput Math Appl* 2010;60:1088–104.
 - [33] Alfi A. Chaos suppression on a class of uncertain nonlinear chaotic systems using an optimal H1 adaptive PID controller. *Chaos Solitons Fractals* 2012;45:351–7.
 - [34] Pérez-Polo MF, Molina MP, Chica JG, Galiano JAB. Stability and chaotic behavior of a PID controlled inverted pendulum subjected to harmonic base excitations by using the normal form theory. *Appl Math Comput* 2014;232:698–718.
 - [35] Narendra KS, Annaswamy AM. *Stable adaptive systems*. Englewood Cliffs, NJ: Prentice-Hall; 1989 [ISBN: 978-0138399948].
 - [36] Tao G. *Adaptive control design and analysis* New Jersey: John Wiley & Sons, Inc.; 2003 [ISBN: 978-0-471-27452-0].
 - [37] Wu F, Lu B. Anti-windup control design for exponentially unstable LTI systems with actuator saturation. *Syst Control Lett* 2004;52:305–22.
 - [38] Rossler OE. An equation of continuous chaos. *Phys Lett* 1976;57A:397–8.